ELSEVIER

Catalysis Today 36(1997) 497–510

CATALYSIS TODAY

Selectivity in heterogeneous catalytic processes

M.V. Landau[a,*], S.B. Kogan[a], D. Tavor[a], M. Herskowitz[a], J.E. Koresh[b]

[a] *The Blechner Center for Industrial Catalysis and Process Development, Ben-Gurion University of the Negev, Beer-Sheva, Israel*
[b] *Nuclear Center Negev, Beer-Sheva, Israel*

Abstract

The selectivity of several catalytic systems was studied. Shape selectivity of Pt on carbon-fiber catalysts was demonstrated in the competitive hydrogenation of 1-hexene and cyclohexene and in the parallel dehydrogenation of cyclohexanol to cyclohexanone and phenol. Both reactions were carried out in a gas-phase fixed-bed reactor. Catalysts prepared on carbon fibers, containing pores with small constrictions (5 Å) yielded significantly higher rates of hydrogenation of 1-hexene compared to those of cyclohexene and selectively produced cyclohexanone from cyclohexanol. Other catalysts, supported on carbon fibers with large constrictions (7 Å) or activated carbon, displayed comparable rates of hydrogenation for both reactants and yielded cyclohexanone as well as phenol from cyclohexanol. Nitration of *o*-xylene with nitrogen dioxide was carried out in the gas phase over a series of solid acid catalysts packed in a fixed bed. Several zeolites, supported sulfuric acid, and sulfated zirconia were tested. Zeolite H-β was found to be the most active and selective catalyst for the production of 4-nitro-*o*-xylene. A preliminary kinetic model indicated that the selectivity to 4-nitro-*o*-xylene increased with decreasing concentration of nitrogen dioxide. Alkylation of phenol with methanol was performed on zeolites, supported sulfuric and phosphoric acids, and sulfated zirconia packed in a fixed-bed. The ratio of *o*- to *c*-alkylation, measured at 180°C and methanol to phenol feed molar ratio of unity, ranged from 4 with the supported acids to 2 with zeolite H-β. This ratio decreased with temperature. The ratio of *o*- to *p*-cresol changed from about 2 in zeolites in supported sulfuric acid and to 0.5 in phosphoric acid supported on carbon fibers.

Keywords: Molecular sieve, carbon; Hydrogenation; Gas phase nitration; Alkylation; Zeolite

1. Introduction

An analysis of the chemical equilibrium composition in systems of organic reactants normally indicates that a large number of reactions are possible. However, in most cases, only one or a limited number of products are desired. Most of the potential by-products have a detrimental effect on the feasibility and operability of a particular process. Selectivity determines the yield of the desired product as well as the yield of waste that has to be disposed. Both yields have a significant effect on the economics of processes. Environmental regulations are a major driving force for improving selectivity [1,2]. Prevention of pollution is required in the development of new processes. Therefore, the selectivity is a key factor in the evaluation of chemical organic processes.

Catalysts are a determining factor in the kinetics of chemical reactions, thus affecting the selectivity of chemical processes directly. An important case is the development of enantioselective catalysts [3]. The extensive research on selectivity of catalysts ranged

*Corresponding author.

PII S0920-5861(96)00240-4

from fundamental studies of test reactions to applications in industrial processes. Recent monographs have been devoted specifically to the different aspects of selectivity in catalysis [4], especially selective oxidation [5–7]. Additional effects on selectivity in catalytic processes like reaction solvents [8] and operating conditions [9] were reviewed recently. This paper presents the study of selectivity in three different heterogeneous catalytic systems.

Catalysts prepared on the basis of zeolites displayed shape selectivity in industrial petroleum, petrochemical and chemical processes [10,11]. Extensive work has been conducted on fundamental and applied aspects of their catalytic properties [10,11]. In contrast, only a limited number of studies have been published on the application of molecular sieve carbon (MSC), in the form of carbon fibers or carbon granules, as supports for catalysts. Fundamental studies [12,13] have shown that the pore dimensions of ultramicroporous carbons could be gradually increased in the 3–6 Å range. Molecules that differ by 0.2 Å in their smallest dimension were separated efficiently by selective adsorption. Hence, MSC provides unique properties to act as shape-selective supports: the possibility of tailor-design constrictions to fit the molecules involved in the selective process and the essentially neutral nature of the carbon support. A recent review [14] described the catalytic properties of MSC based on the limited published literature.

Nitration of aromatic compounds is an industrial process, performed with a mixture of nitric and sulfuric acid, in which a slight molar excess of concentrated nitric acid in respect to the organic compound is used. Environmental problems related to the waste produced in the process and the poor selectivity in the production of alkyl-nitroaromatic compounds promoted the evaluation of other nitrating agents and solid acids. The literature published on this topic has been reviewed recently [15].

One of the viable option to produce alkyl-nitroaromatic compounds is the gas-phase nitration with nitrogen dioxide. Most publications that describe such reaction systems appear in the patent literature. A fundamental study published recently [17,40] communicated results that describe the nitration of several substituted aromatic compounds with nitrogen dioxide, performed on ZSM-5, H-β zeolites and silica–alumina catalysts. The mechanisms proposed in these two papers are contradictory. According to [40], a solid-acid catalyst activated NO_2 as a result of its interaction with Brønsted sites forming NO_2^+ and nitrous acid:

$$N_2O_4 \rightarrow 2NO_2 + H^+\text{-cat}^- \rightarrow NO_2^+ + HNO_2 + \text{cat}^-$$

The aromatic hydrocarbon *Ar*H was subsequently converted to $ArNO_2$ by classical electrophilic attack of NO_2^+ that did not require activation of *Ar*H at the catalysts surface:

$$ArH + NO_2^+ + \text{cat}^- \rightarrow ArNO_2 + H^+\text{-cat}^-$$

But the kinetic measurements published since [16] provide evidence for reaction of the gaseous nitrating agent with the chemisorbed aromatic substrate. Furthermore, the measured catalyst activities in the nitration of various hydrocarbons with different substituents in the aromatic ring did not correlate with the proton affinities of the substrates. This is not consistent with the electrophilic attack mechanism.

A one-electron transfer mechanism through the formation of an aromatic radical cation at the catalyst surface and subsequent recombination of this radical cation with $NO_2\cdot$ radicals from the gas phase was proposed [16]:

$$\text{cat-O}\cdot + ArH \rightarrow \text{cat-O}^- - ArH\cdot^+$$

$$\text{cat-O}^- - ArH\cdot^+ + NO_2\cdot \rightarrow ArNO_2 + \text{cat-OH}$$

The problem is how the protonic-acid sites, responsible for catalytic nitration of *Ar*H by NO_2 [16,40] could form the adsorbed $ArH\cdot^+$ cation radicals. It was proposed that this could take place as a result of the transformation of the Brønsted-acid sites into corresponding surface radicals by abstraction of hydrogen atoms from surface hydroxyls via reaction with $NO_2\cdot$ radicals:

$$\text{cat-OH} + NO_2\cdot \rightarrow \text{cat-O}\cdot + HNO_2$$

Both mechanisms were based on the assumption that nitrous acid was formed. However, it was mentioned [16,17] that nitrous acid was not found in the product. Therefore, oxygen was made to act as one of the reactants that yielded nitrogen dioxide after acid dehydration:

$$2HNO_2 \rightarrow N_2O_3 + H_2O \rightarrow NO\cdot$$

$$+NO_2 \xrightarrow{1/2O_2} 2NO_2\cdot \rightarrow N_2O_4$$

As mentioned in [17], the latter mechanism is unlikely under typical gas-phase nitration conditions, since the generation of radical cations $ArH\cdot^{+}$ require a lot of energy. Therefore, it was proposed that the aromatic ring should be activated most efficiently through the generation of $Ar\cdot$ radicals that can recombine easily with $NO_2\cdot$, thus producing nitro-aromatics ($ArNO_2$) without any intermediate complexes.

In our opinion, the formation of $Ar\cdot$ radicals at the catalyst surface would be possible as a result of abstraction of the hydrogen atom from ArH by surface radicals that could be formed as proposed [16]:

$$\text{cat-O}\cdot + ArH \rightarrow \text{cat-OH} + Ar\cdot$$

leading to regeneration of catalyst sites without the participation of the $NO_2\cdot$ radicals from the gas phase. The problem is that the free-radical mechanism proposed in [17] predicts a close-to-statistical product distribution [16] while the results for solid acids indicate selective production of *para*-nitro-isomers.

The alkylation of phenol with methanol is an important industrial reaction for the production of *o*-cresol and xylenols [18,19]. *o*-Alkylation and *c*-alkylation of the aromatic ring with the potential production of several isomers presents a complex selectivity problem. A large number of studies [20–34] indicate that selectivity is a function of the catalyst type (nature of active sites, Brønsted or Lewis acidic sites and basic sites, their strength and density) and the operating conditions.

The factors that affect the selectivity of phenol alkylation with methanol were investigated recently on γ-alumina, Nafion-H, silica–alumina and supported phosphoric acid [24]. The ratio of *o*- to *c*-alkylation at 200°C increased from 2 for alumina to 5 for silica–alumina and 9 for Nafion-H and supported phosphoric acid. Alumina produced a high ratio of *o*- to *p*-isomers, while the other three catalysts produced a mixture of isomers. The Brønsted-acid sites formed coke, so alumina was deactivated at a much lower rate than the other catalysts. Two mechanisms were invoked to explain the results: adsorption of the aromatic ring on the Brønsted-acid sites or dissociative adsorption of the phenolate ion on the Lewis-acid sites. The former could yield *o*-alkylation on weak sites while the strong sites mostly yield *c*-alkylation. The latter produces either anisole or *o*-cresol.

A series of H-ZSM5 zeolites were employed [25] to examine the effect of Si to Al ratio, diameter of crystallines and aggregates and specific acidity. Anisole was the predominant product with no shape selectivity to *p*-cresol. The lack of shape selectivity was attributed to the dominant contribution of the external active sites. Furthermore, the selectivity to anisole increased with time-on-stream due to the coking of strong external sites that caused rapid deactivation. This effect was further supported by tests of consecutive chlorobenzene and phenol alkylation [34]. The deactivation was related to a strong chemisorption of phenol. The shift in selectivity to anisole as a function of time-on-stream was also confirmed. However, the temperature was found to have the most significant effect on the selectivity [25]. The anisole to cresol ratio increased steeply with decreasing temperature, as the apparent activation energy for the reaction to anisole was estimated to be 10 kcal mol^{-1} compared to 20 kcal mol^{-1} for the reaction to cresol [25].

Screening of several zeolites [21] indicated that H-ZSM5 displayed a very low activity. Zeolite HY yielded a surprisingly high initial selectivity to cresol (53%) compared to that to anisole (9%). The selectivity changed sharply with time-on-stream to 40% for cresol and 50% for anisole after 7 h. Surprisingly, the initial selectivity to xylenols was about 15%.

The purpose of this work is to present results on the selectivity patterns of several catalytic systems. Carbon fibers were tested for potential shape selectivity in hydrogenation and dehydrogenation reactions. Three reactions were selected in this study: hydrogenation of a mixture of 1-hexene and cyclohexene, dehydrogenation of cyclohexane and cyclohexanol. Some of the data were presented elsewhere [35]. The selective nitration of *o*-xylene with nitrogen dioxide to 4-nitro-*o*-xylene was examined on various solid acid catalysts, including a preliminary kinetic analysis of one catalytic system. The alkylation of phenol with methanol was tested with different catalysts, as an example of a complex system that could yield *o*- and *c*-alkylation products with a large number of different isomers.

2. Experimental

The raw material for the carbon-fiber supported catalyst was a fibrous carbon TCM 128 (Carbonne–Lorraine). The supports were obtained by thermochemical treatment with air or carbon dioxide, following a procedure described in [36]. Their surface area calculated from sorption isotherms of carbon dioxide at 298 K, assuming 19.5 $Å^2$ as the CO_2 surface area, was 360 $m^2\ g^{-1}$. The pore volume was 0.15 $cm^3\ g^{-1}$ and the thread diameter was about 1000 nm. Two sets of carbon-fiber supports were used in this study: those with 5 and 7 Å pore diameters in constrictions, as measured by the molecular probe technique [37], termed as CF-S and CF-L, respectively. Pt catalysts were prepared by impregnation of 1–2 g carbon fibers with 4 cm^3 of aqueous solution of H_2PtCl_6 (5% Pt on base of carbon fibers). Following the separation of the solution excess, the samples were dried for 3 h at 50, 100 and 150°C. A different sample, called N2, was prepared by treating 1 g of sample N1 with 2 cm^3 of water for 15 min at 25°C. An Rh-supported catalyst, called N5, was prepared by sublimation. Sample N6 was a catalyst, ESCAT 28, manufactured by Engelhard, having 0.5% Pt on activated carbon granules. The metal catalysts were characterized by XRF and XRD. Their properties are listed in Table 1.

The composition of catalysts tested in the nitration of *o*-xylene, most of them zeolites, are listed in Table 2. All catalysts were 20–40 mesh granules prepared by pressing powder, except silica and HY that were purchased as 1.5 mm extrudates. The supported sulfuric-acid catalyst was prepared by impregnation of silica extrudates with 98% sulfuric acid, using an incipient wetness method. The two samples of H-mordenite zeolites were prepared by decationation/dealumination of Na-mordenite with HCl. The sulfated zirconia was activated by calcination at 550°C in nitrogen. All other catalysts were used as received, with no change in their composition.

Table 1
Characteristics of carbon-fiber catalysts

Sample	Support	Pt (wt%)	Crystallinity (%)	Pt crystal ∅ (nm)
N1	CF-S	1.9	0	<3
N2	CF-S	1.7	10	8
N3	CF-S	0.5	0	<3
N4	CF-L	2.5	0	<3
N5	CF-S	12.6 *	10	19
N6	Activated C	0.5	0	<3

* Active metal is rhodium.

The catalysts tested in the alkylation of phenol are listed in Table 3. Zeolites were purchased in powder and extrudate forms. The powder catalysts were pressed, crushed and sieved to the desired average size. Sulfated zirconia was calcined at 550 and 650°C. Sulfuric acid-on-silica preparation was described above. Phosphoric acid-on-carbon fibers was prepared according to procedures described in [38]. XRD and SEM were used to determine the crystallinity and Si to Al ratio of zeolites. TPD with ammonia was used to determine the acidity of the catalysts.

The carbon-fiber supported catalysts were tested in a stainless-steel, 17 mm i.d. and 300 mm long, fixed-bed reactor, equipped with an electric heater and packed with 0.5 g of catalyst. The organic reactant was fed to a vaporizer by an Eldex metering pump, in parallel with hydrogen, controlled by a Brooks mass

Table 2
Composition of nitration catalysts

Sample	Catalyst	Composition (wt%)				
		SiO_2	Al_2O_3	Na_2O	ZrO_2	H_2SO_4
S-1	H-ZSM5	96.7	3.2	0.05		
S-2	H-ZSM5	98.3	1.6	0.05		
S-3	H-β	96.7	3.2	0.05		
S-4	H-mordenite	98.4	1.6	0.01		
S-5	H-mordenite	99.0	1.0	0.01		
S-6	HY	98.3	1.6	0.03		
S-7	Sulfated zirconia				95	5
S-8	H_2SO_4/silica	70				30

Table 3
Composition and properties of alkylation catalysts

Sample	Type of catalyst	Supplier	SiO_2/Al_2O_3	Cation, acid (wt%)	Surface area ($m^2\ g^{-1}$)	Original particle form	Crystallinity (%)
Y1	HY	Linde	6.8	Na_2O-2.4	660	Powder	
Y2	HY	PQ	12	Na_2O-0.19	730	1.6 mm	82
Y3	HY	PQ	60	Na_2O-0.13	720	1.6 mm	76
Y4	HY	PQ	60		720	Powder	40
Y5	LaY	PQ	5.1	La_2O-25.7 Na_2O-1.7		Powder	
Y6	CaY	PQ	6.2	Na_2O-2.5 CaO-18.5		Powder	
ZS1	HZSM-5		30	Na_2O-1.0	430	Powder	55
ZS2	HZSM-5	PQ	50	Na_2O-1.8	420	Powder	
ZS3	HZSM-5	PQ	90	Na_2O-0.76	450	Powder	
B1	H-β	PQ	25		730	Powder	60
M1	H-mordenite	PQ	16.9	Na_2O-0.44	450	Powder	59
Z1	SO_4^{2-}/ZrO_2	MEL			90	Powder	
S1	H_2SO_4 on SiO_2	SiO_2 from PQ		H_2SO_4-30		1.6 mm	
P1	H_3PO_4 on carbon			H_3PO_4-35		Fiber	

flowmeter. The mixture flowed to the reactor and the effluent was vented. The temperature in the vaporizer and the reactor was controlled by Eurotherm controllers and measured by thermocouples inserted in 6 mm-o.d. thermowells. Gas samples were withdrawn from the effluent and analyzed by GC. All experiments were carried out at atmospheric pressure to measure the initial performance of the catalyst over periods of up to 8 h.

Nitration of *o*-xylene with nitrogen dioxide was carried out in a glass, 20 mm i.d. and 300 mm long tubular reactor, cooled by circulating an oil in the jacket and packed with 15 g of catalyst. *o*-Xylene was fed to a glass vaporizer by an Eldex metering pump. Nitrogen dioxide flowed through a Brooks flow controller to a preheater and to the reactor through a separate inlet to reduce the contact with *o*-xylene prior to the contact with the catalyst bed. Nitrogen used as a diluent was fed through a Brooks flowmeter. In some experiments, nitrogen was replaced by air. The product was condensed and analyzed by GC.

The phenol alkylation experiments were carried out in a stainless steel, 14 mm-i.d. reactor, equipped with a 6 mm-o.d. thermowell and an electric heater. Catalysts in amounts of 1–3 g were diluted with equal volumes of silica and were packed between layers of glass rings. Temperature measurements along the catalyst bed indicated isothermal conditions within 2°C. Mixtures of phenol and methanol were fed by a syringe pump at rates ranging from 5.0 to 5.9 g h^{-1} through a preheater kept at the same temperature as in the reactor. The products were collected in a glass trap maintained at −5 to +4°C, depending on the feed composition. Nitrogen, the carrier gas, was fed at volumetric rates of 0.03–0.2 NLM. Analysis of liquid reactants and products, *o*-, *m*-, *p*-cresol, anisole, *o*-, *m*-, *p*-methyl anisole, all xylenol isomers and dimethyl ether was carried out by GC.

3. Results and discussion

3.1. Shape selectivity of molecular sieve carbons

The hydrogenation of the 1-hexene and cyclohexene mixture (1:1 molar ratio) yielded hexane and cyclohexane. Rates of reaction, calculated from low conversion (5–10%) data measured at 100°C, WHSV=25–50 h^{-1} and hydrogen to organic reactant molar ratio of 10, are listed in Table 4. The difference in selectivity, defined as the ratio of the reaction rates of hexene and cyclohexene, between the samples N4 and N6 on one hand, and N3 on the other, is very significant. This difference is attributed to the shape selectivity of the N3 samples, as illustrated in Fig. 1 by the high conversion data.

Table 4
Rates and selectivities of hydrogenation reactions

Catalyst	Reaction rate (mol (g Pt)$^{-1}$ h^{-1})		Selectivity
	1-Hexene (r_1)	Cyclohexene (r_2)	r_1/r_2
N3	22	8	2.8
N4	86	79	1.1
N6	46	40	1.1

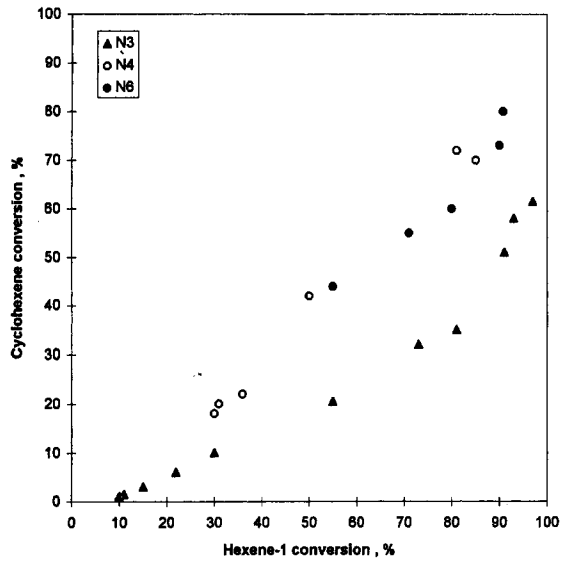

Fig. 1. Shape selectivity of carbon fibers in cyclohexene and hexene hydrogenation measured at similar operating conditions.

The dehydrogenation of cyclohexane on catalysts N1, N2 and N5 yielded <5% conversion over the temperature range 300–400°C, WHSV=20 h^{-1}, hydrogen to organic reactant molar ratio of 3. At similar operating conditions and 300°C, the conversion with catalyst N6 was 39%. The apparently low activity of the carbon-fiber supported catalysts, in spite of the high concentration of active metal sites, could be explained by the configurational diffusion resistance inside the narrow constrictions that were further blocked by metal atoms.

A critical test of this specific behavior of the carbon-fiber catalysts was performed with cyclohexanol, where a clear distinction could be made between the reaction of the OH group and the reaction of the ring. Little cracking to hydrocarbons was expected since the carbon support was not acidic. The conversion of cyclohexanol and the molar selectivity to the two main products, phenol and cyclohexanone, and the hydrocarbon by-products are listed in Table 5. A clear and sharp difference in the performance of the four catalysts tested was recorded.

Table 5
Conversion and selectivities of cyclohexanol dehydrogenation

Catalyst	Temperature (°C)	Conversion (%)	C-one (%)	HC (%)	Phenol (%)
N1	300	3	93	7	0
	350	12	92	8	0
	400	25	95	3	2
N2	300	14	98	1	1
	350	34	92	2	6
	400	43	80	2	18
N5	300	14	98	1	1
	350	34	95	4	1
	400	40	88	7	5
N6	300	9	40	5	55
	350	18	22	1	77
	400	27	20	2	78

In contrast to the results of the cyclohexane dehydrogenation, the conversion measured with the carbon-fiber catalysts N2 and N5 were higher than that with catalyst N6. Catalysts N1 and N6 yielded comparable conversions. The reason becomes apparent considering the high selectivity to cyclohexanone. The main reaction was the dehydrogenation of the small OH group due to its access to the active sites. Interestingly, catalyst N2, that was water washed, yielded a higher activity and lower selectivity compared to that of catalyst N1. It indicates that this method made the active sites more accessible to the ring, thus, increasing conversion and reducing selectivity. This is probably due to back migration of the Pt compound to the external surface and formation of crystals, as indicated in Table 1.

3.2. *Nitration of o-xylene with nitrogen dioxide*

Four parameters were measured as an index of performance: the conversion of *o*-xylene, the selectivity to 4-nitro-*o*-xylene (S_{4n}), the selectivity to oxy-

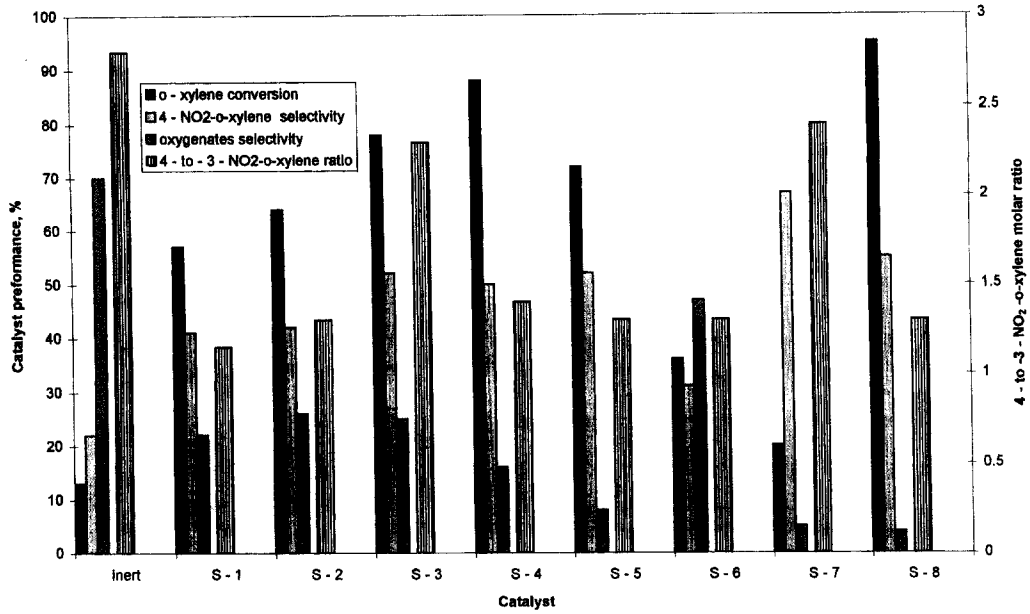

Fig. 2. Performance of catalysts in the nitration of *o*-xylene: T=130°C (50°C for S-3 and S-8); *o*-xylene WHSV = 0.1 h^{-1}; NO_2 GHSV = 80 h^{-1}; and N_2 GHSV = 200 h^{-1}.

genates (S_o) and the molar ratio of 4- to 3-nitro-*o*-xylene (R_{43}). The selectivity was defined as the ratio between the molar rate of the specific product to the molar rate of converted *o*-xylene. The homogeneous reaction measured in the reactor packed with glass rings was found to be significant at the operating conditions selected for testing the catalysts, as shown in Fig. 2. The main reaction in the experiments performed with inert packing was found to be the oxidation of *o*-xylene, characteristic of a free-radical mechanism. Similar results were reported for toluene [15,17]. The nitration rates were relatively low.

A wide range of conversions, 19–92%, were measured at *o*-xylene WHSV=0.1 h^{-1}, NO_2 to *o*-xylene molar ratio of 7, total partial pressure of reactants of 0.31 atm and 130°C. No dinitrogen tetraoxide is expected at those conditions, based on the analysis of chemical equilibrium [39]. The reaction temperature was reduced to 50°C with the most active catalysts, H-β and supported sulfuric acid, to limit the conversion to <95%. At those conditions, NO_2 is in equilibrium with N_2O_4, as indicated by a detailed thermodynamic analysis of this system given in Ref. [39]. Starting the reactor at temperatures >70°C caused extensive runaways. Temperatures reached levels >800°C within a few seconds as expected in complete oxidation of *o*-xylene. Therefore, particular care was taken in the experiments with the two active catalysts.

No dinitro-xylene products were detected. Replacing nitrogen with air did not change the conversion and the selectivity. It means that oxygen played no role in the nitration with nitrogen dioxide, in contradiction with data reviewed in Ref. [17], that yielded a higher conversion. This could be a result of the minor effect of the oxidation step on the overall reaction rates.

H-β and sulfated zirconia displayed considerably higher values for R_{43}, close to 2.5, well above about 1.5 displayed by all other catalysts. The wide pores of the H-β zeolite could be a reason for the performance different from other zeolites. However, most of the reaction could have taken place on the external surface of the crystals, as found in other reaction systems [40]. The sulfated zirconia, a catalyst that combines Lewis- and Brønsted-strong-acid sites [41], was much less active than all other Brønsted-type catalysts.

The performance of the H-β and supported sulfuric acid catalysts was further tested as a function of *o*-xylene WHSV and its concentration. The results, plotted in Fig. 3, indicate that the 4-nitro-*o*-xylene

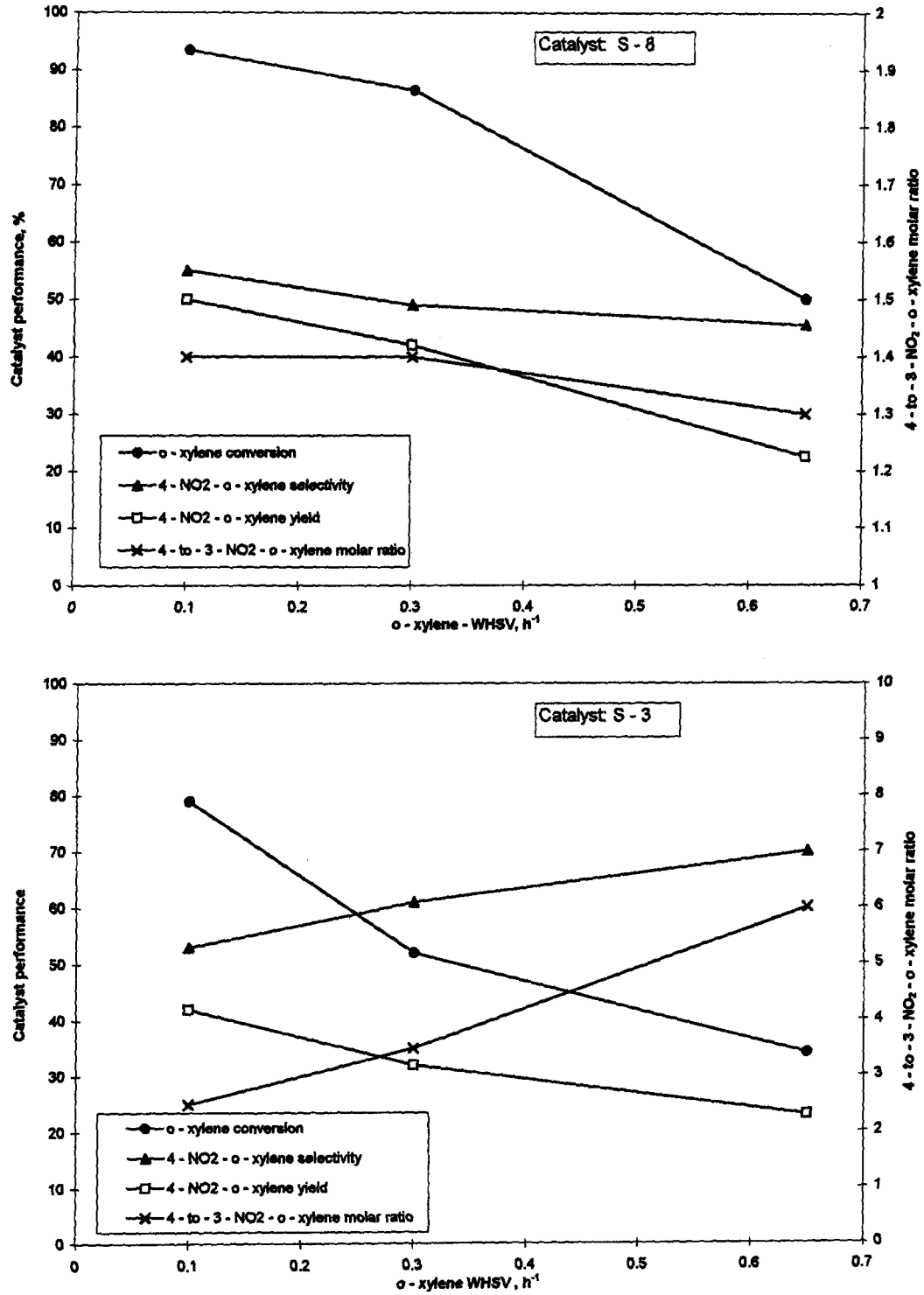

Fig. 3. Effect of *o*-xylene weight hourly space velocity on the catalysts performance at 50°C. Operating conditions are listed in the legend to Fig. 2.

Table 6
Kinetic data for nitration of *o*-xylene with dinitrogen tetraoxide

$WHSV_{o\text{-xyl}}$ (h^{-1})	Xylene feed mole fraction	NO_2 feed mole fraction	4-Nitro-*o*-xylene yield	3-Nitro-*o*-xylene yield	Phthalic anhydride yield
0.1	0.047	0.165	0.18	0.030	0.039
0.1	0.042	0.222	0.23	0.064	0.064
0.1	0.039	0.273	0.40	0.17	0.19
0.1	0.036	0.317	0.42	0.26	0.23
0.3	0.108	0.259	0.33	0.10	0.09
0.65	0.208	0.191	0.24	0.04	0.05

selectivity and the ratio of 4- to 3-nitro-*o*-xylene increased with decreasing *o*-xylene conversion up to 70% on the H-β catalyst. They remained approximately constant on the supported sulfuric acid.

A quantitative analysis of the performance of the H-β catalyst at 50°C was carried out based on preliminary kinetic measurements, listed in Table 6. Three reactions were considered in the kinetic model:

$$o\text{-}C_8H_{10} + N_2O_4 \Rightarrow 4\text{-}C_8H_9NO_2 + HNO_2 \quad (1)$$

$$o\text{-}C_8H_{10} + N_2O_4 \Rightarrow 3\text{-}C_8H_9NO_2 + HNO_2 \quad (2)$$

$$o\text{-}C_8H_{10} + 1.5N_2O_4 \Rightarrow C_8H_6O_4 + 1.5N_2 + 2H_2O \quad (3)$$

Only the main oxidation product, phthalic anhydride, was accounted for. Power-law kinetic expressions for the three reactions were assumed. Mass balances for the three products were expressed in the form:

$$\frac{dY_i}{d(1/WHSV)} = k_i\left(1 - \sum_{i=1}^{3} Y_i\right)^{\alpha_i} y_4^{\beta_i} y_{50}^{\alpha_i}, \quad i = 1, 2 \text{ and } 3 \quad (4)$$

where Y_1, Y_2 and Y_3 are the yields of 4-nitro-*o*-xylene, 3-nitro-*o*-xylene and phthalic anhydride, respectively; y_4, the mole fraction of N_2O_4 in the gas phase calculated from a differential mass balance combined with an algebraic equation that accounts for chemical equilibrium; y_{50}, the mole fraction of *o*-xylene in the feed; k_i, the rate constants; and α_i and β_i, the reaction orders with respect to *o*-xylene and NO_2 for each one of the reactions.

The parameters were estimated using the SIMULSOLV software. A parity plot shown in Fig. 4 indicates a reasonable agreement between the experimental and the calculated values. The reaction order with respect to *o*-xylene was estimated to be close to zero (α_1=0.2, α_2=0.2 and α_3=0.1). This is in agreement with the results reported for fluorobenzene [16]. No kinetic data have been reported for *o*-xylene. The reaction order with respect to NO_2 was estimated to be: $\beta_1 = 1.3$, $\beta_2 = 2.1$ and $\beta_3 = 1.7$. Our results agree with the model [16] that described the activation of the aromatic substrate at the catalyst surface, followed by reaction with NO_2 from gas phase: zero-order for *o*-xylene is evident of its strong adsorption at the catalysts surface while the significant effect

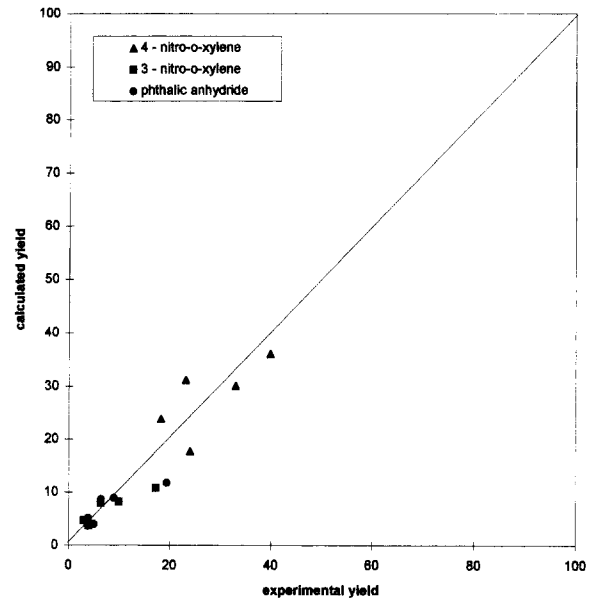

Fig. 4. Comparison of calculated and experimental nitration data.

of the NO_2 concentration in gas phase on the reaction rate could be a result of its reaction with strongly adsorbed *Ar*H. The adsorption of *o*-xylene to form the intermediate active species for the production of 3-NO_2-*o*-xylene is sterically hindered by the adjacent methyl group. This could differentiate between the interaction of the adsorbed 3-C· with 4-C· xylene radicals, with the nitrogen dioxide radical thus affecting selectivity and yielding a different reaction order. The variation in selectivity could be related to the different orientation of the adsorbed active species relative to the cat-O· radicals on the S-7 and S-8 catalyst surface or in bulk of zeolite crystals.

These results indicate that the selectivity to 4-nitro-*o*-xylene increased with lower concentrations of nitrogen dioxide. This implies that operating at low partial pressures of nitrogen dioxide would significantly increase the selectivity. However, considering the high dependency of the rate on nitrogen dioxide, the space velocity of *o*-xylene needs to be decreased at these conditions to maintain the same conversion.

3.3. *Alkylation of phenol with methanol*

The proper design of the trap, combined with the detailed analysis of the liquid reactants and products, yielded a good material balance. In most experiments, >95% of the reactant's feed mass was recovered as liquid in the trap. The detailed composition of the product in five sample runs is listed in Table 7. Phenol was converted up to about 30%, mostly to cresols and anisole. The methanol side reaction to dimethyl ether was negligible. In the few experiments, carried out with a methanol feed mole fraction of 0.58, the methanol conversion to dimethyl ether reached about 10%. HZSM-5 catalysts, applied in the dehydration of methanol to dimethyl ether, produced a low yield of dimethyl ether, probably because of the strong adsorption of phenol.

Intrapellet mass transfer had little effect on the initial performance of the catalysts. Tests performed with catalyst Y1, with three pellet sizes over the 0.5–1.5 mm range, yielded a similar initial phenol conversion and product selectivity. Deactivation measured for periods ranging 1.5–4 h was observed in certain cases. Relatively high deactivation rates were observed with the largest pellets. HZSM-5 zeolites at temperatures as low as 180°C, HY zeolites and sulfated zirconia displayed relatively high deactivation rates at 300°C, while H-β was relatively stable, as illustrated in Fig. 5. No significant changes in selectivity were measured as a function of time-on-stream, as illustrated for sulfated zirconia in Fig. 6.

Table 7
Product composition in alkylation runs [a]

	Catalyst				
	B1	M1	Y4	ZS1	Z1
Phenol conversion (mol%)	29.0	10.9	22.1	30.6	23.0
Selectivity (mol%)					
Anisole	28.2	41.4	32.0	34.5	52.3
o-Cresol	36.5	22.9	32.3	36.2	27.1
m-Cresol	11.2	10.4	10.1	10.9	5.5
p-Cresol	18.2	17.6	21.0	14.4	11.6
o-Methylanisole	0.7	0.7	1.5	0.9	0.0
m-Methylanisole	4.2	5.7	3.3	1.7	3.1
p-Methylanisole	0.0	0.0	0.0	0.3	0.0
2,6-Dimethylphenol	0.1	0.0	0.0	0.5	0.4
Other xylenols	0.0	0.0	0.0	0.5	0.0
Mass balance (wt%)	95	98	93	96	94
o-Cresol/*p*-cresol	2.20	1.30	1.54	2.51	2.34
m-Cresol/*p*-cresol	0.62	0.59	0.48	0.76	0.47

[a] Temperature 300°C; phenol to methanol molar ratio 2:1; nitrogen flow 0.21 NLM; and phenol WHSV = 1.8 h^{-1}.

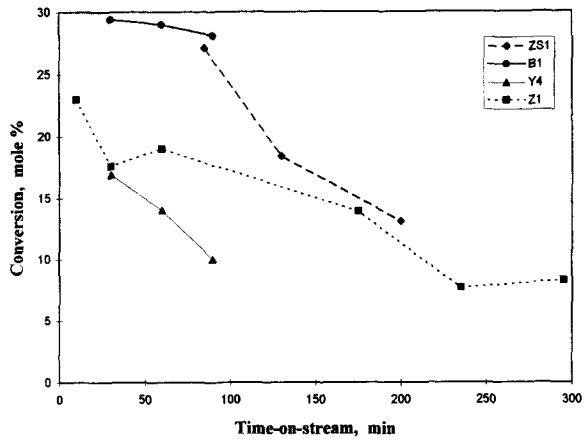

Fig. 5. Deactivation patterns of catalysts in alkylation of phenol.

Catalyst	Phenol WHSV (h^{-1})	Temperature (°C)	Phenol/methanol molar ratio
ZS1	2	180	1
B1	4.3	300	1
Y4	4.3	300	1
Z1	1.8	300	2

Operating conditions: T=180°C, phenol to methanol molar ratio !;!, phenol WHSV=2 h^{-1}.

A comparison of the performance of catalysts at 180°C is listed in Table 8. All data represent the initial activity to avoid masking effects of deactivation. The activity of zeolites HZSM-5 and HY decreased with the increasing ratio of Si to Al. The selectivity to *o*-alkylation increased gradually. Furthermore, the ratio

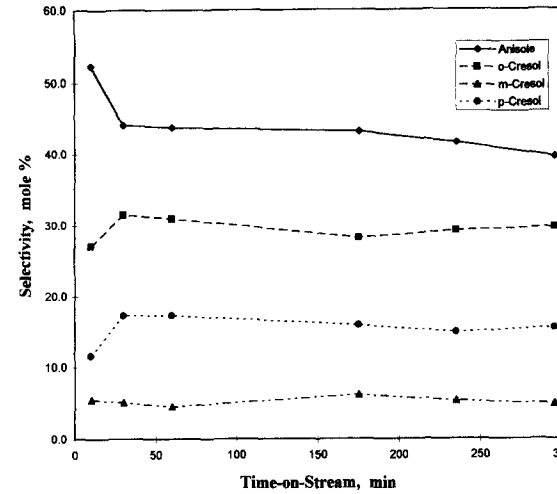

Fig. 6. Selectivity of catalyst Z1 as a function of time-on-stream. Operating conditions are listed in the legend to Fig. 5.

of *o*- to *p*-cresol was close to 2, as expected if electrophilic substitution is assumed [30,31]. Introduction of the cations, lanthanum or calcium, reduced the phenol conversion and the *o*-alkylation significantly. The ratio of *o*- to *p*-cresol shifted to about unity. Catalyst H-β performed similarly to HZSM-5 and HY catalysts. No shape-selectivity effects were observed. The lack of such effects are attributed to the dominant contribution of external active sites, as reported for this reaction [31] and for other reaction systems [41].

Table 8
Results of catalyst testing [a]

Type of catalyst	Conversion of phenol (%)	Selectivity (mol%)				
		Anisole	*o*-Cresol	*m*-Cresol	*p*-Cresol	Others
Y1	29.0	68.1	16.0	4.2	9.6	2.1
Y2	27.0	73.7	9.8	9.2	3.2	4.1
Y4	19.7	77.5	9.7	6.8	5.0	1.0
Y5	16.0	57.3	18.2	7.5	16.0	1.0
Y6	16.6	61.7	17.1	5.7	14.2	1.3
ZS1	27.1	71.4	15.1	2.4	8.5	2.6
ZS2	23.0	80.0	10.3	3.0	6.3	0.4
ZS3	16.1	78.4	11.5	2.9	7.0	0.2
B1	22.4	65.6	16.3	4.7	10.4	3.0
M1	5.1	55.0	18.3	9.4	15.6	1.7
S1	24.5	79.6	9.6	2.9	7.8	0.1
P1	11.3	82.7	4.6	3.3	9.4	0.0

[a] Temperature, 180°C; phenol to methanol molar ratio, 1:1; and phenol WHSV=2 h^{-1}.

H-mordenite yielded a considerably different performance. Its activity was much lower, while the selectivity to *o*-alkylation was somewhat lower compared with other zeolites. The reason could be shape selectivity, although no direct evidence is available at this point.

Supported sulfuric acid yielded, as expected, a high ratio of *o*- to *c*-alkylation. The *o*- to *p*-cresol ratio was close to unity, probably because of geometric factors in adsorption. Particularly significant are the results obtained on phosphoric acid supported on carbon fibers. The conversion was small and the *o*- to *c*-alkylation ratio was high due to the low strength of acid sites, but the *o*- to *p*-cresol ratio was about 0.5, probably as a result of shape selectivity.

The effect of operating conditions on performance was also tested. Increasing temperature increased the *c*- to *o*-alkylation ratio, shown in Fig. 7, in agreement with previous results [27,30,31]. The conversions at the two temperatures were about the same, probably as a result of extensive deactivation at 500°C. The distribution of cresols was also affected by temperature. Both *m*- and *p*-cresol increased with increasing temperature. The methanol feed concentration was varied over a wide range (4–58 mol%), while the phenol concentration was kept constant at 9 mol%. Increasing the methanol feed concentration by a factor of two increased the conversion by almost 50% for the H-β catalyst, as shown in Fig. 8. Further increase in the methanol feed concentration by a factor of five increased the conversion by only about 25%. The conversion in experiments with zeolite HY, plotted in Fig. 9, was almost independent of methanol concentration. A significant difference in the selectivity was measured with zeolites H-β and HY. The ratio of

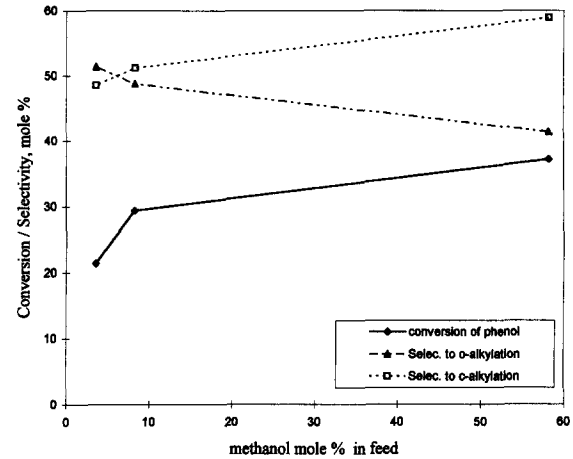

Fig. 8. Effect of methanol concentration on the B1 catalyst performance

Methanol in feed (mol%)	3.6	8.3	58.2
Phenol WHSV (h^{-1})	4.9	4.3	2.0

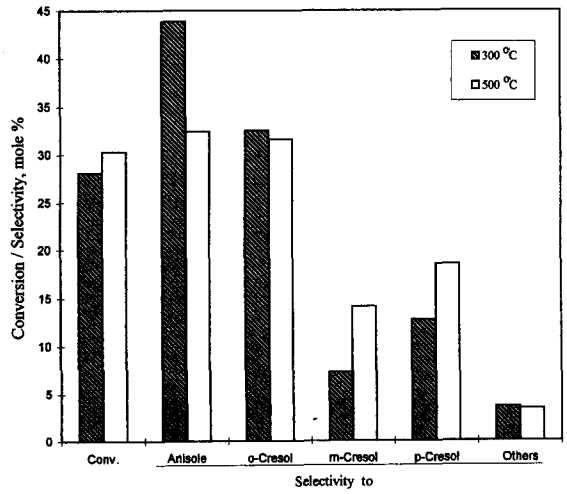

Fig. 7. Effect of temperature on the B1 catalyst performance. Operating conditions are listed in the legend to Fig. 5.

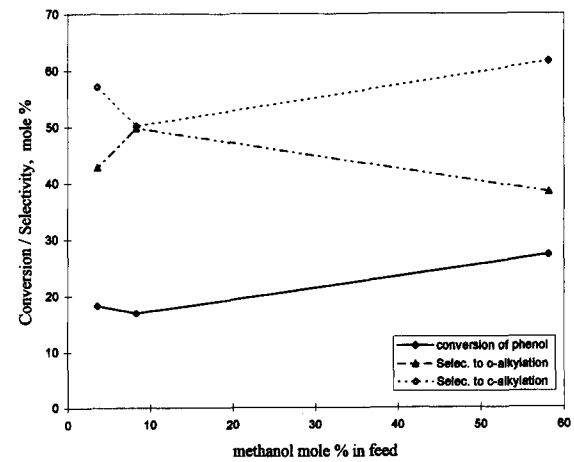

Fig. 9. Effect of methanol concentration on the Y4 catalyst performance. Operating conditions are listed in the legend to Fig. 8.

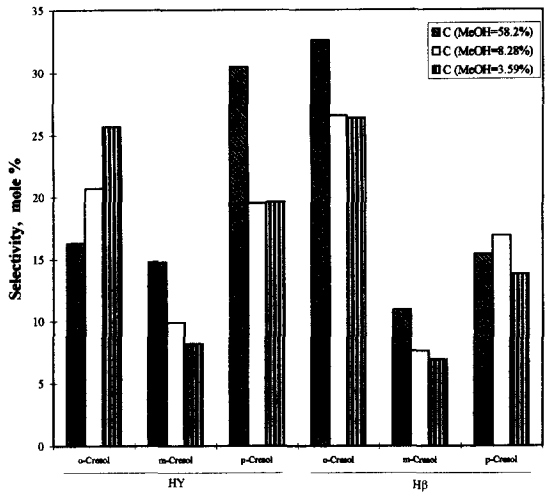

Fig. 10. Effect of methanol concentration on the cresol isomer distribution. Operating conditions are listed in the legend to Fig. 8.

o- to *c*-alkylation decreased with increasing methanol concentration on the former, while a maximum value was measured on the latter. Particularly interesting is the opposite trend in the distribution of cresols, illustrated in Fig. 10. Selectivity to *o*-cresol increased with methanol concentration for H-β and decreased for HY. The *o*- to *p*-cresol ratio decreased from 1.3 to 0.5, while it remained at about 2 as the methanol mole fraction in the feed increased from 3.6% to 58% with HY and H-β zeolites, respectively.

Sulfated zirconia contains a combination of Lewis and Brønsted acid sites [42]. It has been suggested that the strong acidity of the catalyst originates from the presence of both Lewis and Brønsted sites [43]. Interestingly, the *c*- to *o*-alkylation ratio was about the same as for other zeolites. Furthermore, this ratio increased with time-on-stream, implying that there was faster deactivation of sites responsible for *o*-alkylation.

4. Conclusions

The selectivity was studied in three catalytic systems. Several novel catalysts were examined together with commercial catalysts. Shape selectivity of carbon-fiber-supported catalysts was demonstrated in two reactions:

- rate of hydrogenation of 1-hexene was three times higher than the rate of cyclohexene hydrogenation on Pt, supported on carbon fibers containing small constrictions (5 Å), while similar rates for the two reactions were measured with Pt, supported on carbon fibers containing large constrictions (7 Å) and activated carbon; and
- dehydrogenation of cyclohexanol that yielded cyclohexanone selectively (>90%) on the catalysts containing Pt and Rh on small-constriction carbon fibers, while a mixture of phenol and cyclohexanone was obtained with Pt on activated carbon.

Nitration of *o*-xylene with nitrogen dioxide yielded a significantly higher selectivity compared to that of nitric acid. Among the large number of catalysts, zeolites and acid supported catalysts, H-β yielded the best performance. Its activity was high, thus limiting the reaction temperature to 70°C. Higher temperatures caused runaways. No dinitro-*o*-xylene compounds were detected. The ratio of 4- to 3-nitro-*o*-xylene reached values as high as 6, while nitration with nitric acid normally yields a ratio lower than unity. A preliminary kinetic model of this system, accounting for the nitration to the 4- and 3-nitro-isomers and oxidation to the main by-product, phthalic anhydride, was developed. Decreasing the nitrogen dioxide partial pressure increases the selectivity to 4-nitro-*o*-xylene.

Zeolites did not display shape selectivity in the alkylation of phenol with methanol, although similar catalysts yielded *p*-xylene from toluene selectively. Little effect of zeolite type (HY, HZSM-5 and H-β) and the Si to Al ratio on selectivity was recorded. At 180°C, *o*- to *c*- alkylation ratio was close to 2 and about the same was the *o*- to *p*-cresol ratio. Introduction of cations increased the *c*- to *o*-alkylation ratio and the *p*- to *o*-cresol ratio. H-mordenite displayed an extremely low activity. Supported sulfuric acid on silica and phosphoric acid on carbon fibers yielded *o*- to *c*-alkylation ratios as high as 5. The *p*- to *o*-cresol ratio reached a value of 2 with the latter catalyst, implying shape selectivity. The two supported acid catalysts, although different in their strength, displayed a rather similar selectivity pattern, different from the performance of the zeolites. Sulfated zirconia, that contains strong Lewis and Brønsted acids, displayed significant deactivation at 300°C but did not show a different selectivity pattern compared with the zeolites.

Increasing temperature decreased the *o*- to *p*-alkylation ratio down to unity at 300°C and to about 0.5 at 500°C, as expected from the stronger dependency of *c*-alkylation on temperature. Increasing the methanol to phenol ratio by one order of magnitude, from 0.5 to 5, had little effect on selectivity.

References

[1] K.G. Hancock, in P.T. Anastase and C.A. Farris (Eds.), Benign by Design, Am. Chem. Soc., Symp. Ser., 577 (1993) 23.

[2] L.E. Manzer, in P.T. Anastase and C.A. Farris (Eds.), Benign by Design, Am. Chem. Soc., Symp. Ser., 577 (1993) 144.

[3] H.U. Blaser and M. Muller, in M. Guisnet (Ed.), Studies in Surface Science and Catalysis, Vol. 59, Elsevier, Amsterdam, 1991.

[4] M.E. Davis and S.L. Suib (Eds.), Selectivity in Catalysis, Am. Chem. Soc., Symp. Ser., 517 (1993).

[5] V. Cortes Corberan and S. Vic Bellon (Eds.), Stud. Surf. Sci. Catal., 82 (1994).

[6] G. Centi and F. Trifiro (Eds.), Stud. Surf. Sci. Catal., 55 (1990).

[7] S.T. Oyama and J.W. Hightower (Eds.), Catalytic Selective Oxidation, Am. Chem. Soc. Symp. Ser., 523 (1993).

[8] L. Gilbert and C. Mercier, in M. Guisnet (Ed.), Studies in Surface Science and Catalysis, Vol. 78, Elsevier, Amsterdam, 1993.

[9] I.R. Feins and S. Spronck in M.G. Scaros and M.L. Prunier (Eds.), Catalysis of Organic Reactions, Marcel Dekker, New York, NY, 1995.

[10] H. van Bekkum, E.M. Flanigen and J.C. Jansen (Eds.), Stud. Surf. Sci. Catal., 58 (1991).

[11] G.A. Olah and A. Molnar, Hydrocarbon Chemistry, John Wiley and Sons, New York, NY, 1995.

[12] J.E. Koresh and A. Soffer, J. Chem. Soc. Faraday I, 76 (1980) 2457.

[13] J.E. Koresh and A. Soffer, J. Chem. Soc. Faraday I, 76 (1980) 2472.

[14] H.C. Foley, Microporous Mater., 4 (1995) 407.

[15] G.A. Olah, R. Malhotra and S.C. Narang, Nitration. Methods and Mechanisms, VCH Publishers, New York, NY, 1989.

[16] A. Germain, T. Akouz and F. Figueras, J. Catal., 147 (1994) 163.

[17] L.V. Malysheva, E.A. Paukshtis and K.G. Ione, Catal. Rev. Sci. Eng., 37 (1995) 179.

[18] K. Weissermel and H.J. Arpe, Industrial Organic Chemistry, 2nd edn., VCH, Weinheim, 1993.

[19] H. Fiege, Ullmann's Encyclopedia of Industrial Chemistry, 8 (1987) 25.

[20] R. Pierantozzi and A.F. Nordquist, Appl. Catal., 21 (1986) 263.

[21] S. Balsama, P. Beltrame, P.L. Beltrame, P. Carniti, L. Forni and G. Zuretti, Appl. Catal., 13 (1984) 161.

[22] P.D. Chantal, S. Kaliaguine and J.L. Grandmaison, Appl. Catal., 18 (1985) 133.

[23] M. Renaud, P.D. Chantal and S. Kaliaguine, Can. J. Chem. Eng., 64 (1986) 787.

[24] E. Santacesaria, D. Grasso, D. Gelosa and S. Carra, Appl. Catal., 64 (1990) 83.

[25] E. Santacesaria, M. Di Serio, P. Ciambelli, D. Gelosa and S. Carra, Appl. Catal., 64 (1990) 101.

[26] J. Kaspi and G.A. Olah, J. Org. Chem., 43 (1978) 3142.

[27] R.F. Parton, J.M. Jacobs, H.V. Ootenghemand, P.A. Jacobs, in H.G. Karge and J. Weitkamp (Eds.), Studies in Surface Science and Catalysis, Vol. 46, Zeolites as Catalysts, Sorbents and Detergent Builders, Elsevier, Amsterdam, 1989.

[28] N.S. Chang, C.C. Chen, S.J. Chu, P.Y. Chen and T.K. Chuang, in H.G. Karge and J. Weitkamp (Eds.), Studies in Surface Science and Catalysis, Vol. 46, Zeolites as Catalysts, Sorbents and Detergent Builders, Elsevier, Amsterdam, 1989.

[29] Z.H. Fu and Y. Ono, Catal. Lett., 21 (1993) 43.

[30] K. Tanabe, M. Misono, Y. Ono and H. Hattori, Studies in Surface Science and Catalysis, Vol. 51, New Solid Acids and Bases, Elsevier, Amsterdam, 1989.

[31] T.K. Li, I. Wang and K.R. Chang, Ind. Eng. Chem. Res., 32 (1993) 1007.

[32] M. Marczewski, J.P. Bobido, G. Perot and M. Guisnet, J. Mol. Catal., 50 (1989) 211.

[33] M.C. Samolada, E. Grigoriadou, Z. Kiparissides and I.A. Vasalos, J. Catal., 152 (1995) 52.

[34] M.R. Goldwasser, L. Garcia, G. Gianetto, M. Guisnet and P. Magnoux, in Catalysis of Organic Reactions, Marcel Dekker, New York, NY, 1995.

[35] S. Kogan, M.V. Landau, M. Herskowitz and J.E. Koresh, Stud. Surf. Sci. Catal., 78 (1991) 353.

[36] J.E. Koresh and A. Soffer, J. Chem. Soc. Faraday I, 77 (1981) 3005.

[37] J.E. Koresh, J. Chem. Soc. Faraday I, 89 (1993) 2059.

[38] S.B. Kogan, M. Herskowitz and J.E. Koresh, Israeli Patent App. 116121 (1995).

[39] S.I. Sandler, Chemical and Engineering Thermodynamics, 2nd edn., John Wiley and Sons, New York, NY, 1989.

[40] N.F. Salakhutdinov, K.G. Ione and E.A. Kobzar, Zh. Organich. Khim., 29 (1993) 546.

[41] X. Song and A. Sayari, Chemtech, 25(8) (1995) 27.

[42] P. Nascimento, C. Akratopoulou, M. Oszagayan, G. Coudurier, C. Travers and J.C. Vedrine, Stud. Surf. Sci. Catal., 1185 (1993) 75.

[43] A. Crearfield, G.P.D. Serrette and A.H. Khazi-Syed, Catal. Today, 20 (1994) 295.